Journal of Coordination Chemistry
Publication details, including instructions for authors and subscription information:
http://www.tandfonline.com/loi/gcoo20

Synthesis, characterization, EDX, thermal, antioxidant, antibacterial, topographical, and gas adsorption studies of supramolecular tetraammoniumplatinate

R.K. Ameta [a], Man Singh [a] & R.K. Kale [a]
[a] School of Chemical Sciences, Central University of Gujarat, Gandhinagar, India
Accepted author version posted online: 17 Jan 2013.Published online: 21 Feb 2013.

To cite this article: R.K. Ameta, Man Singh & R.K. Kale (2013) Synthesis, characterization, EDX, thermal, antioxidant, antibacterial, topographical, and gas adsorption studies of supramolecular tetraammoniumplatinate, Journal of Coordination Chemistry, 66:4, 551-567, DOI: 10.1080/00958972.2013.763230

To link to this article: http://dx.doi.org/10.1080/00958972.2013.763230

Journal of Coordination Chemistry
Vol. 66, No. 4, 20 February 2013, 551–567

Synthesis, characterization, EDX, thermal, antioxidant, antibacterial, topographical, and gas adsorption studies of supramolecular tetraammoniumplatinate

R.K. AMETA, MAN SINGH* and R.K. KALE

School of Chemical Sciences, Central University of Gujarat, Gandhinagar, India

(*Received 14 August 2012; in final form 11 October 2012*)

Reaction of K_2PtCl_4 with N-alkyl-N-benzyl-N,N-dimethyl ammonium chloride ($n = 8$, 10, 12 and 14 for alkyl) yielded supramolecular bis(benzyldimethylalkylazaniumyl) tetrachloroplatinumdiuide (metallobenzalkonium8 (MBK8), MBK10, MBK12, MBK14) characterized with spectroscopic and energy dispersive X-ray techniques. X-ray difraction powder analysis was performed which confirmed the crystalline nature of the compound. UV/Vis study performed in dimethylformamide, dimethylsulphoxide (DMSO)/H_2O, and DMSO/phosphate buffers under physiological conditions show stability of the supramolecular units, $[(C_6H_5CH_2N(CH_3)_2(C_nH_{2n+1})]_2^+$ with $[PtCl_4]^{2-}$. Zeta potential with particle size distribution of MBK8 obtained with DLS-confirmed agglomeration of the coordinate units. Thermal analysis by differential scattering calorimetric showed an effect of alkyl chain on their heat retention. For MBK8, topographical analysis and specific surface area were investigated with atomic force microscopy and nitrogen adsorption method, illustrating an outstanding alignment in arrays of ionic units, and an extent of apparent cross-sectional areas, respectively. Antioxidant and antibacterial activities were determined with 1–2,5-diphenyl-2-picrylhydrazyl-scavenging effect and Gram-positive and Gram-negative bacteria, respectively. The compounds exhibited activities for both scavenging and bacteria.

Keywords: MBK; Adsorption; Antioxidant; Biological activity

1. Introduction

Platinum-based halide salts (Magnus green and derivatives) have been of interest in material sciences, solid state, and catalyst chemistry with significant historical importance [1–16]. These are potent occupational sensitizing agents capable of inducing hypersensitivity in refineries [17]. Many platinum salts have been studied for their effects on the production of IgE antibody to unrelated antigens, such as ovalbumin in adjuvant primed animals [18]. Magnus green salt is a quasi-1-D $[Pt(NH_3)_4][PtCl_4]$ compound comprising linear arrays of platinum(II) both cationic and anionic. Recently, soluble and processable derivatives of Magnus salt have been synthesized by substituting ammonia with linear and branched amino alkanes [19]. In this article, we replaced the cationic part by a quaternary ammonium group where electrostatic communications between oppositely charged coordination units led to stacking of the coordination units of salt into a quasi-1-D structure, rather than bond formation as in Magnus salt [1,20,21–37].

*Corresponding author. Email: mansingh@cug.ac.in

Journal of Coordination Chemistry
ISSN 0095-8972 print/ISSN 1029-0389 online
http://dx.doi.org/10.1080/00958972.2013.763230

Salts of quaternary ammonium bases (QAB) are traditionally considered as effective extracting agents for metals of the platinum group [38], used for metal extraction through an anion exchange mechanism [39–42]. The chosen QAB (Benzalkonium Chloride, BKC) as cationic part of $[(C_6H_5CH_2N(CH_3)_2(C_nH_{2n+1})]_2^+$ $[PtCl_4]^{2-}$ units are broad-spectrum antimicrobial agents [43]. BKC is frequently used as a preservative in several available ophthalmic aqueous/non-aqueous solutions, nebulizer compounds, and nasal sprays. It is a cationic detergent whose surface-active configuration is accountable for its rapid and prolonged incorporation into cell lipid membranes [44]. The same features of BKC make it useful as disinfectants, biocides, and detergents, but also as antielectrostatics of phase transfer catalysts [45]. BKC is bactericidal and antimicrobial with changes of n-alkyl chain length enhancing antimicrobial activity; for example, the C12-homolog is most effective against yeast and fungi, the C14-homolog against Gram-positive bacteria and C16-homolog against Gram-negative bacteria [46]. BKC is widely accepted as preservatives for ophthalmic, parenteral products, and disinfectants for medical equipment [47–50]. It may be considered for efficacy trials in the reduction of mother to child transmission of HIV, possibly in combination with other compounds, such as short course antiretroviral prophylaxis whose efficacy has been demonstrated [51].

Synthesis of supramolecular compounds of tetrachloroplatinate with BKC could lead to further advances in medical sciences, pharmaceutical, nanotechnology, industrial progressions, and others. Square-planar PtX_4 assemblies (X = Cl, Br) are classical Werner-type transition metal complexes [52,53]. They are involved in a number of catalytic reactions and have been extensively studied [54–69]. Developing metallic supramolecular compounds with properties of platinum (anticancer) and BKC (potential antimicrobial, antiviral, antifungal activities) may advance medicinal and industrial fields [70]. Despite the possibilities of QAB incorporating tetrachloroplatinate, there are no reports on ionic supramolecular frameworks of tetrachloroplatinate with the BKC. Thus, studies on bis(benzyldimethylalkylazaniumyl) tetrachloroplatinumdiuide comprising [n-C_8H_{17}-n-$C_6H_5CH_2$,-n, n-$(CH_3)_2N]_2[PtCl_4]$, [n-$C_{10}H_{21}$-n-$C_6H_5CH_2$-n,n-$(CH_3)_2N]_2[PtCl_4]$, [n-$C_{12}H_{25}$-n-$C_6H_5CH_2$-n, n-$(CH_3)_2N]_2[PtCl_4]$, and [n-$C_{14}H_{29}$-n-$C_6H_5CH_2$-n,n-$(CH_3)_2N]_2[PtCl_4]$ having hydrophobic and hydrophilic domains may develop useful molecules.

2. Experimental

2.1. *Materials and methods*

Potassium tetrachloroplatinate (K_2PtCl_4, 99.99%) and BKCs (>99.5%) were procured from Sigma Aldrich. Milli-Q water was used as solvent. The complexes were identified by FT-IR (Perkin Elmer) in KBr plates with polystyrene thin film as calibration standard. Powder X-ray difraction (XRD) patterns were taken by XRD, PTS 3000 by Rich-Seifert. Elemental analyzes were performed with the Euro vector instrument. ^{1}H NMR spectra were recorded in $CDCl_3$ (NMR grade, 99.99%) with a Bruker-Biospin Avance-III 500 MHz FT-NMR. For chemical shifts, TMS was used as the internal standard. Mass spectra were measured on an Agilent Q-TOP LC/MS with both modes. In ESI+ mode, acetonitrile and water were in 3:7 ratios as mobile phase, and in ESI−ve mode, aqueous ammonium acetate (100 mM) and acetonitrile were used in 1 : 11 ratio. Qualitative analyzes for Pt, Cl, N, and C were conducted with SEM–Energy Dispersive X-ray (EDX).

2.2. *General consideration for synthesis*

Synthesis of metallobenzalkoniums (MBKs) using K_2PtCl_4 and BKC in 1 : 2 ratio was performed in nitrogen. The aqueous solutions were separately prepared for K_2PtCl_4 in 15 ml of water and BKC in 15 mL water. The BKC solution was added to the K_2PtCl_4 solution dropwise with stirring (500 rpm). On addition of the BKC solution, the platinum salt precipitated, but on increasing the stirring to 1200 rpm, the precipitate disappeared. The mixture after 16 h produced a light pink precipitate which was filtered off and washed with water and ethanol several times separately and dried in a vacuum oven overnight. The compounds were powders and insoluble in water and ethanol, slightly soluble in acetonitrile and completely soluble in chloroform, dimethylformamide (DMF) and dimethylsulphoxide (DMSO).

2.2.1. Bis(benzyldimethyloctylazaniumyl)tetrachloroplatinumdiuide. Two hundred milligrams of K_2PtCl_4 (0.48 mmol) and 284.9 mg (0.96 mmol) octylbenzalkoniumchloride were taken separately. Anal. calcd for $C_{34}H_{60}N_2Cl_4Pt$ (%): C, 48.98; H, 7.25; N, 3.36. Found: C, 48.88; H, 7.12; N, 3.30. Spectral data: **FTIR** (KBr): ν (–CH_3) 3034.7, 3014, 2989.8 cm^{-1}, ν(–CH_2) 2953, 2928, 2855.1 cm^{-1}, ν(Ar–CH) 883.67 cm^{-1}, ν(mono substitute Ar) 785.71, 720.4, 704.08 cm^{-1}, ν(C–N) 1218.4, 1165.3 cm^{-1}, ν(Pt – N) 520.4, 451.02 cm^{-1}. **^{1}H NMR** ($CDCl_3$): δ 0.890–0.864 (t, J = 13.00 MHz, 3H, $CH_2CH_2C\mathbf{H_3}$), 1.334–1.246 (m, 8H, $(CH_2)_4$), 1.459–1.417 (m, 2H, $CH_2C\mathbf{H_2}CH_3$), 1.868 (m, 2H, $C\mathbf{H_2}CH_2N^+$), 3.598 (s, 6H, $(CH_3)_2N^+$), 3.85–3.822 (t, J = 16 MHz, 2H, CH_2N^+); 5.217 (s, 2H, $PhC\mathbf{H_2}N^+$), 7.436 (s, 3H, Ph), 7.842–7.832 (d, J = 4.5 MHz, 2H, Ph). The +ve **ESI-MS**: m/z 248.2390 [M^+] (calc. for $[C_{17}H_{30}N]^+$ = 248.44), **–ve ESI-MS:** m/z 389.6122 [M-1 + NH_4Cl] (calc. for [$PtCl_4$ + NH_4Cl] = 390.381). **UV/Vis** in DMF: λ_{max} [ε ($dm^3mol^{-1}cm^{-1}$)] = 260 (1443), 335 (179.5), 400 (135.5) nm, in DMSO: water (1 : 1): λ_{max} [ε ($dm^3mol^{-1}cm^{-1}$)] = 270 (1611), 335 (263) nm, in DMSO: phosphate buffer (1 : 1): λ_{max} [ε ($dm^3mol^{-1}cm^{-1}$)] = 255 (1146), 305 (184.5) nm.

2.2.2. Bis(benzyldimethyldecylazaniumyl)tetrachloroplatinumdiuide. Two hundred milligrams of K_2PtCl_4 (0.48 mmol) and 299.4 mg (0.96 mmol) decylbenzalkoniumchloride were taken separately. Anal. calcd for $C_{38}H_{68}N_2Cl_4Pt$ (%): C, 51.29; H, 7.70; N, 3.15. Found: C, 51.21; H, 7.62; N, 3.10. Spectral data: **FTIR** (KBr): ν(–CH_3) 3071.4, 3018.4, 2977.6 cm^{-1}, ν(–CH_2) 2953, 2924.5, 2855.1 cm^{-1}, ν(Ar–CH) 871.43 cm^{-1}, ν(mono substitute Ar) 777.55, 732.65, 704.08 cm^{-1}, ν(C–N) 1218.4, ν(Pt – N) 557.14, 479.6, 451.02 cm^{-1}. **^{1}H NMR** ($CDCl_3$): δ 0.907–0.880 (t, J = 13.5 MHz, 3H, $CH_2CH_2C\mathbf{H_3}$), 1.335–1.247 (m, 12H, $(CH_2)_6$), 1.473–1.415 (m, 2H, $CH_2C\mathbf{H_2}CH_3$), 1.867 (m, 2H, $CH_2CH_2N^+$), 3.597 (s, 6H, $(CH_3)_2N^+$), 3.842–3.809 (t, J = 16.5 MHz, 2H, $C\mathbf{H_2}N^+$), 5.212 (s, 2H, $PhC\mathbf{H_2}N^+$), 7.439 (s, 3H, Ph),7.836–7.827 (d, J = 4.5 MHz, 2H, Ph). **ESI-MS:** m/z 276.2703 [M^+] (calc. for $[C_{19}H_{34}N]^+$ = 276.50). **–ve ESI-MS:** m/z 389.6122 [M-1 + NH_4Cl] (calc. for [$PtCl_4$ + NH_4Cl] = 390.381). **UV/Vis** in DMF: λ_{max} [ε ($dm^3mol^{-1}cm^{-1}$)] = 260 (1398), 335 (12.5), 400 (82.5) nm, in DMSO: water (1 : 1): λ_{max} [ε ($dm^3mol^{-1}cm^{-1}$)] = 260 (1159.5), 355 (193) nm, in DMSO: phosphate buffer (1 : 1): λ_{max} [ε ($dm^3mol^{-1}cm^{-1}$)] = 255 (1159.5), 305 (193) nm.

2.2.3. Bis(benzyldimethyldodecylazaniumyl)tetrachloroplatinumdiuide. Two hundred milligrams of K_2PtCl_4 (0.48 mmol) and 327.4 mg (0.96 mmol) dodecylbenzalkoniumchloride

were taken separately. Anal. Calcd for $C_{42}H_{76}N_2Cl_4Pt$ (%): C, 53.33; H, 8.10; N, 2.96. Found: C, 53.26; H, 8.01; N, 2.89. Spectral data: **FTIR** (KBr): ν(–CH_3) 3067.3, 3022.4 cm^{-1}, ν(–CH_2) 2916.3, 2851 cm^{-1}, ν(Ar−CH) 875.51 cm^{-1}, ν(mono substitute Ar) 781.63, 732.65, 704.08 cm^{-1}, ν(C–N) 1218.4, ν(Pt – N) 557.14, 479.6 cm^{-1}. **^{1}H NMR** ($CDCl_3$): δ 0.914–0.887 (t, J = 13.5 MHz, 3H, $CH_2CH_2C\mathbf{H_3}$), 1.329–1.244 (m, 16H, $(CH_2)_8$), 1.453–1.425 (m, 2H, $CH_2C\mathbf{H_2}CH_3$), 1.863 (m, 2H, $CH_2C\mathbf{H_2}N^+$), 3.598 (s, 6H, $(CH_3)_2N^+$), 3.843–3.81 (t, J = 16.5 MHz, 2H, $C\mathbf{H_2}N^+$), 5.218 (s, 2H, $PhC\mathbf{H_2}N^+$), 7.435 (s, 3H, Ph), 7.841–7.832 (d, J = 4.5 MHz, 2H, Ph). **ESI-MS:** *m/z* 304.3025 [M^+] (calc. for $[C_{21}H_{38}N]^+$ = 304.55). **–ve ESI-MS:** *m/z* 389.6122 [M-1 + NH_4Cl] (calc. for [$PtCl_4$ + NH_4Cl]=390.381). **UV/Vis** in DMF: λ_{max} [ε ($dm^3mol^{-1}cm^{-1}$)] = 260 (1080.5), 335 (52.5), 400 (42.5) nm, in DMSO: water (1 : 1): λ_{max} [ε ($dm^3mol^{-1}cm^{-1}$)] = 270 (1699), 335 (261.5) nm, in DMSO: phosphate buffer (1 : 1): λ_{max} [ε ($dm^3mol^{-1}cm^{-1}$)] = 260 (1310), 305 (254.5) nm.

2.2.4. Bis(benzyldimethyltetradecylazaniumyl)tetrachloroplatinumdiuide. Two hundred milligrams of K_2PtCl_4 (0.48 mmol) and 389.3 mg (0.96 mmol) tetradecylbenzalkoniumchloride were used. Anal. Calcd for $C_{46}H_{84}N_2Cl_4Pt$ (%): C, 55.14; H, 8.45; N, 2.80. Found: C, 55.06; H, 8.33; N, 2.71. Spectral data: **FTIR** (KBr): ν(–CH_3) 3034.7 cm^{-1}, ν(–CH_2) 2920.4, 2855.1 cm^{-1}, ν(Ar–CH) 895.92 cm^{-1}, ν(mono substitute Ar) 789.8, 724.49, 704.08 cm^{-1}, ν(C–N) 1218.4, ν(Pt – N) 524.49, 451.02 cm^{-1}. **^{1}H NMR** ($CDCl_3$): δ 0.913–0.886 (t, J = 163.5 MHz, 3H, $CH_2CH_2C\mathbf{H_3}$), 1.316–1.270 (m, 20H, $(CH_2)_{10}$), 1.411–1.382 (m, 2H, $CH_2C\mathbf{H_2}CH_3$), 1.836 (m, 2H, $C\mathbf{H_2}CH_2N^+$), 3.580 (s, 6H, $(CH_3)_2N^+$), 3.846–3.814 (t, J = 16 MHz, 2H, $C\mathbf{H_2}N^+$), 5.213 (s, 2H, $PhC\mathbf{H_2}N^+$), 7.405 (s, 3H, Ph), 7.858–7.848 (d, J = 5, 2H, Ph). ESI-MS: *m/z* 332.2014 [M^+] (calc. for $[C_{23}H_{42}N]^+$ = 332.61). **–ve ESI-MS:** *m/z* 389.6122 [M-1 + NH_4Cl] (calc. for [$PtCl_4$ + NH_4Cl]=390.381). **UV/Vis** in DMF: λ_{max} [ε ($dm^3mol^{-1}cm^{-1}$)] = 260 (1269), 335 (106), 400 (67) nm, in DMSO: water (1 : 1): λ_{max} [ε ($dm^3mol^{-1}cm^{-1}$)] = 270 (1577.5), 335 (239.5) nm, in DMSO: phosphate buffer (1 : 1): λ_{max} [ε ($dm^3mol^{-1}cm^{-1}$)] = 255 (1184), 305 (187.5) nm.

2.3. *UV/Vis spectroscopy*

Electronic spectra were recorded with a Spectro 2060 plus model UV/Vis spectrophotometer from 200 to 600 nm using 1 cm path length cuvette. DMF was used for solution preparation. The stability of compounds was determined by preparing a solution in DMSO/water and DMSO/phosphate buffer of pH 7.2. Buffer solution was prepared by adding 70 mL 0.1 M aqueous NaOH solution into 0.1 M aqueous KH_2PO_4 solution. The pH of the resultant buffer was checked with RS-232 modeled Cyber scan pH 2100, EUTECH pH meter instrument. Their concentration for the UV study with DMF, DMSO/water and DMSO phosphate buffer was kept constant at 2×10^{-3} M.

2.4. *Conductance measurement*

Conductance was measured with a LABINDIA, PICO + model conductivity meter at 25 °C for 1×10^{-3} M solution in DMF. Aqueous 0.1 M (12.88 mS/cm), 0.01 M (1.413 mS cm^{-1}) and 0.001 M (147 μS cm^{-1}) KCl solutions were used for calibration standard.

2.5. *Zeta potential and particle size measurement*

A Microtrac Zetatrac, U2771, Dynamic Light Scattering equipment was used for solution prepared in DMSO. Set-zero was done with DMSO, and then, 15% MBK8 in DMSO was

filled in the sample holder. For Zeta potential and particle size standard, an auto-suspended solution of alumina suspension (400206-100) was used.

2.6. *SEM and EDX analysis*

SEM images were obtained with EVO18-18-69 model ZEISS SEM. The sample was adhered to carbon tape and then made conductive in a coater chamber of gold (80%) and palladium (20%) by plasma sputtering. EDX analysis was made for qualitative analysis of the elements (except H, due to an absence of L electron) in compounds with a EVO18-18-69 model ZEISS SEM.

2.7. *Differential Scanning Calorimetry (DSC)*

Heat-holding capacity was determined with an Intracooler Perkin-Elmer DSC-6000 in an aluminum sample holder with Pyris manager software. The 2 mg sample was taken for measurement at 5 °C min^{-1} heating and cooling rate. Aluminum pen was used as reference and also as sample holder.

2.8. *Atomic force microscopy analysis*

Topographical studies were carried out with a XE-76 model, advanced scanning probe, Park system corp. Atomic force microscopy (AFM) technique was used with silicon cantilever in noncontact taping mode. The 0.1 M solution in chloroform was put on a 10×2.5 cm^2 glass slide, and the chloroform was evaporated in vacuum at room temperature for half an hour. On complete evaporation, it was scanned for topography under set phase and amplitude.

2.9. *Gas adsorption*

Surface area, pore size volume, and pore size distribution determinations were made by sorptomatic with multilayer adsorption with Brunauer, Emmett and Teller (BET) theory, Thermo Scientific (Surfer). MBK8 (478.3 mg) was poured in a burette for degassing overnight at 90 °C with 10^{-2}–10^{-3} torr vacuum. Then, the burette was attached to a liquid N_2 containing Dewar flask at 1.5 bar N_2 gas pressure.

2.10. *Antioxidant activities*

Antioxidant activities were assessed on the basis of free radical scavenging of stable 1-2,5-diphenyl-2-picrylhydrazyl (DPPH). Diluted solutions were prepared in DMSO/water (1 : 1). DPPH (0.002% prepared in DMSO/water, 1 mL) was mixed with 1.5 mL of compound and shaken vigorously and kept in the dark for 30 min. The absorbance was measured at 517 nm with a Spectro 2060 plus model UV/Vis spectrophotometer. Radical-scavenging activity was measured as a decrease in absorbance of DPPH. A lower absorbance of reaction mixture indicated higher free radical-scavenging activity which was calculated with the following formula:

$$\text{Scavenging/activity } \% = (A_0 - A_S/A_0) \times 100$$

with A_S absorbance of DPPH with a test compound and A_0 absorbance of DPPH without a test compound (control). Data for antioxidation are presented as means ± SD of three determinations.

2.11. *Biological evaluation*

The synthesized compounds were screened for their antibacterial activities against human pathogenic bacteria, *viz*. Gram-negative (*Escherichia coli*; ATCC 25922) and Gram-positive (*Staphylococcus aureus*; ATCC 33591) bacterial strains by Kirby Beurs Disc Diffusion Method using DMSO as solvent at 200 μg mL^{-1} on Mueller Hinton Agar media. The zone of inhibition was measured in millimeter (mm) after 24 h incubation at 37 °C and pH 7.4. The zones of inhibition were compared with the standard drugs ampicillin (10 μg) and gentamycin (10 μg) which had resistant and sensitive $\leqslant 28$, $\geqslant 28$ and $\leqslant 12$ and $\geqslant 15$, respectively. Discs with only DMSO were used as positive control.

3. Results and discussion

3.1. *Synthesis and characterization*

Synthesis of MBK was conducted with potassium tetrachloroplatinate (K_2PtCl_4) and N-alkyl-N-benzyl-N,N-dimethyl ammonium chloride (BKC, $n = 8$, 10, 12, and 14 alkyl side chain) in aqueous solution. On mixing and continuous vigorous stirring of BKC and K_2PtCl_4 producing N-alkyl-N-benzyl-N-N-dimethyl ammonium cation and divalent tetrachloroplatinate anion resulted in light pink MBK after 24 h. Four different 99% pure MBK compounds were synthesized with 95% yield (scheme 1). The compounds were not soluble in water, ethanol, and methanol, confirming strong ionic bonds.

The –CH_3- and –CH_2-stretching bands in FTIR of MBK compounds are at 3071–2977 cm^{-1} and 2955–2851 cm^{-1}, respectively. At 895–871 cm^{-1}, aromatic –CH were confirmed. A peak for mono substituted benzene ($PhCH_2$–) was noted at 789–704 cm^{-1}. The C–N bending vibrations were at 1218 cm^{-1}. The platinum nitrogen ionic bond vibration was identified at 524–479 cm^{-1} [71–74].

In ^{1}H NMR of MBKs, H_3, H_4, and H_5 (scheme 1) of the benzene ring of N-alkyl-N-benzyl-N,N-dimethyl ammonium produced a singlet at $\delta = 7.405$–7.439 ppm and (H_2 and H_6 (scheme 1) appeared at 7.858–7.827 ppm as doublets with $J = 4.5$ MHz. Two benzyl –CH_2 protons appeared at 5.21 ppm as a singlet. Six protons of two –CH_3 on quaternary nitrogen showed a singlet at 3.597 ppm. The 2H protons of $CH_2C\mathbf{H_2}N^+$ showed a triplet at 3.85–3.81 with $J = 16$ MHz, due to deshielding by the more electronegative nitrogen.

The 2H of $C\mathbf{H_2}CH_2N^+$ showed a multiplet at 1.86–1.83 ppm, due to an influence of 2H placed nearest to nitrogen (CH_2N^+), and from alkyl protons (8H, 10H, 12H, 14H of MBK8, MBK10, MBK12, MBK14, respectively) with a broad multiplet at 1.316–1.270 ppm. The 2H of $CH_2C\mathbf{H_2}CH_3$ appeared at 1.459–1.382 ppm with multiplets. The –CH_3 of the alkyl chain showed a triplet at 0.914–0.864 ppm with $J = 13$ and 13.5 MHz. The MBKs have ionic bonds; thus the ESI +ve mass spectra showed cationic M^+ mass peaks, 248.2390, 276.2703, 304.3025, and 332.2014 for $[C_{17}H_{30}N]^+$, $[C_{19}H_{34}N]^+$, $[C_{21}H_{38}N]^+$, and

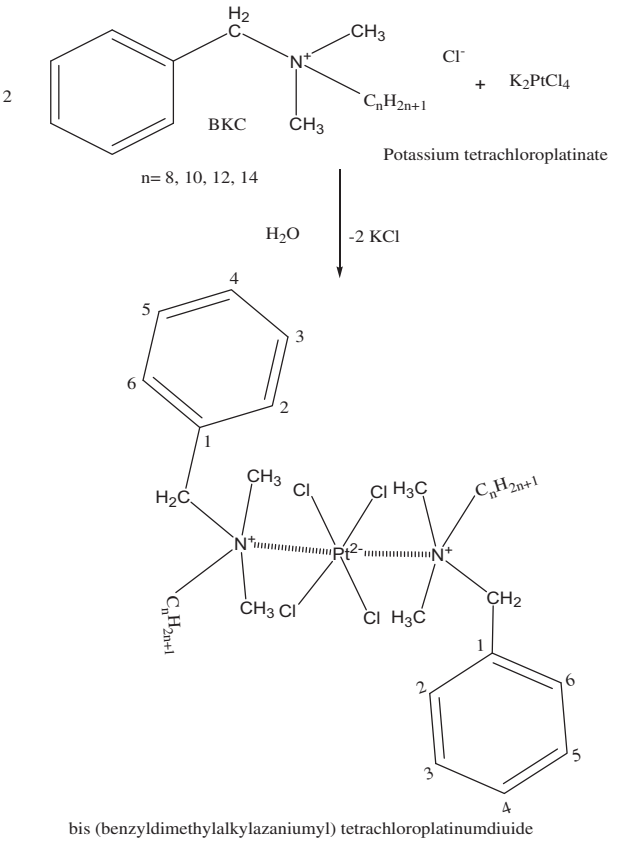

Scheme 1. Reaction scheme 1.

$[C_{23}H_{42}N]^+$, respectively. In the negative mode, they showed M-1 peak having $m/z = 389.61$ for $PtCl_4$ with an additive mass of NH_4Cl ($m/z = 53.491$), due to use of aqueous ammonium acetate as mobile phase in the negative mode.

3.2. *XRD analysis*

XRD powder pattern peaks for MBK8 shown in Supplementary material indicate the crystalline nature of the compound. The highest intensity peak was evaluated at 5.65θ angle with 15.6293A d-spacing value. The full width half maximum value for this peak was 0.1233.

3.3. *Absorption spectroscopy*

UV/Vis spectra were recorded in DMF for 2×10^{-3} molar solution from 200 to 600 nm. The compounds and K_2PtCl_4 exhibit three λ_{max} at 260, 335, and 400 nm (figure 1) and the same patterns of spectra with K_2PtCl_4 showed $PtCl_4^{2-}$ in the compounds. The absorption spectrum consists of a band at 400 nm, assigned as $^1A_{1g} \rightarrow {}^1A_{2g}$ ($d_{xy} \rightarrow d_{x^2-y^2}$) transition [75]. The other d-d bands occurred at higher energies and interacted with quaternary ammonium transitions. Their solutions in DMF produced the same λ_{max}, but decreased in intensity,

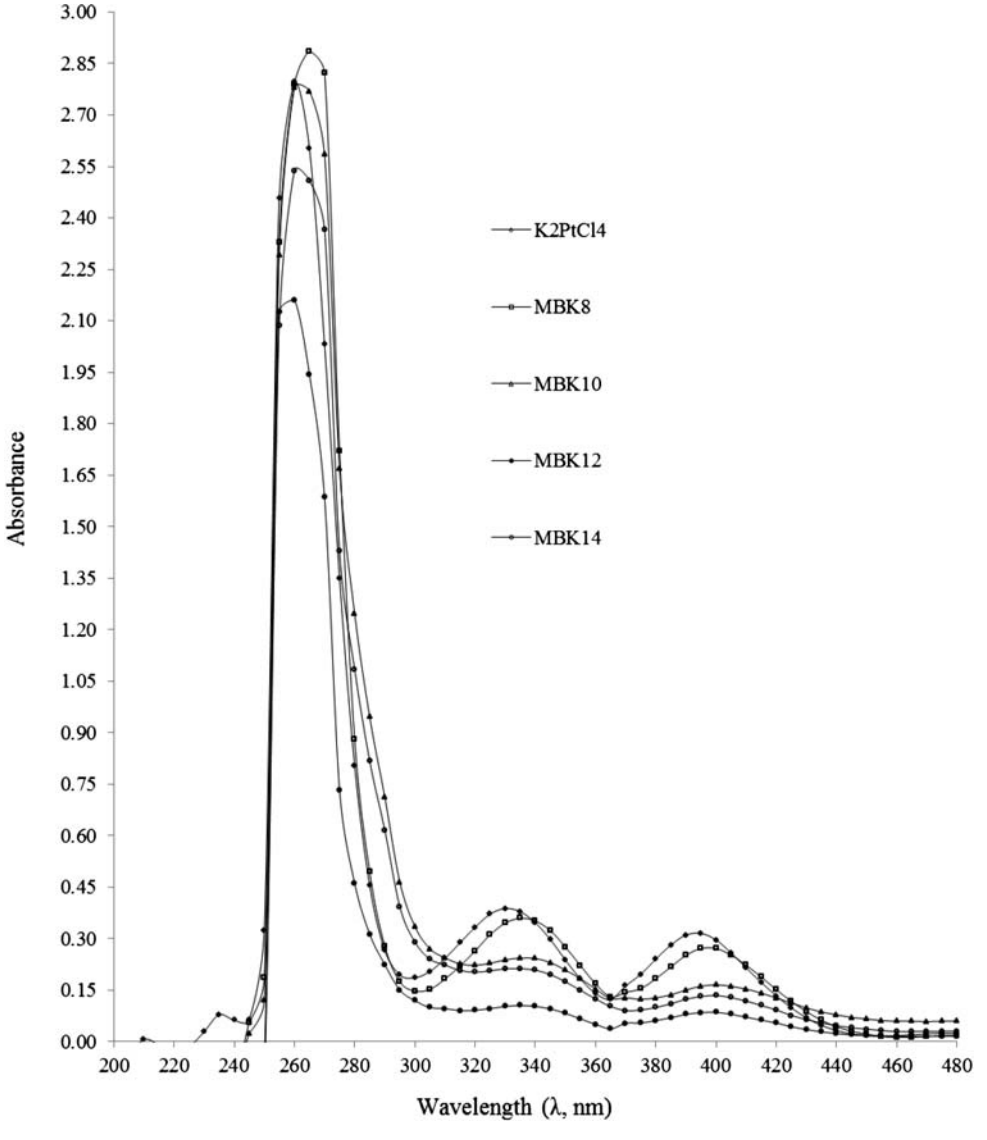

Figure 1. UV/Vis spectra of MBKs in DMF.

and indicated no formation of bond between platinum and nitrogen. A decrease in absorbance inferred charge–charge interaction between Pt^{2-} and positively charged quaternary nitrogen similar to Magnus salts [19]. To investigate whether the solid state structure is retained in solution, the UV/Vis spectral behavior was investigated in DMSO/water as well as in DMSO/phosphate buffer (pH = 7.2) for 2×10^{-3} M (figures 2 and 3). The overall patterns for spectra corresponding to each compound were similar. The compounds including K_2PtCl_4 showed two λ_{max} at 270 and 335 in DMSO/water (figure 2) and at 260 and 305 in DMSO/phosphate buffer (figure 3). The same λ_{max} inferred stability, but a decrease in absorbance of K_2PtCl_4 also informed a charge–charge interaction between Pt^{2-} and the positively charged quaternary nitrogen in DMSO/water and DMSO/phosphate. Such interactions prove

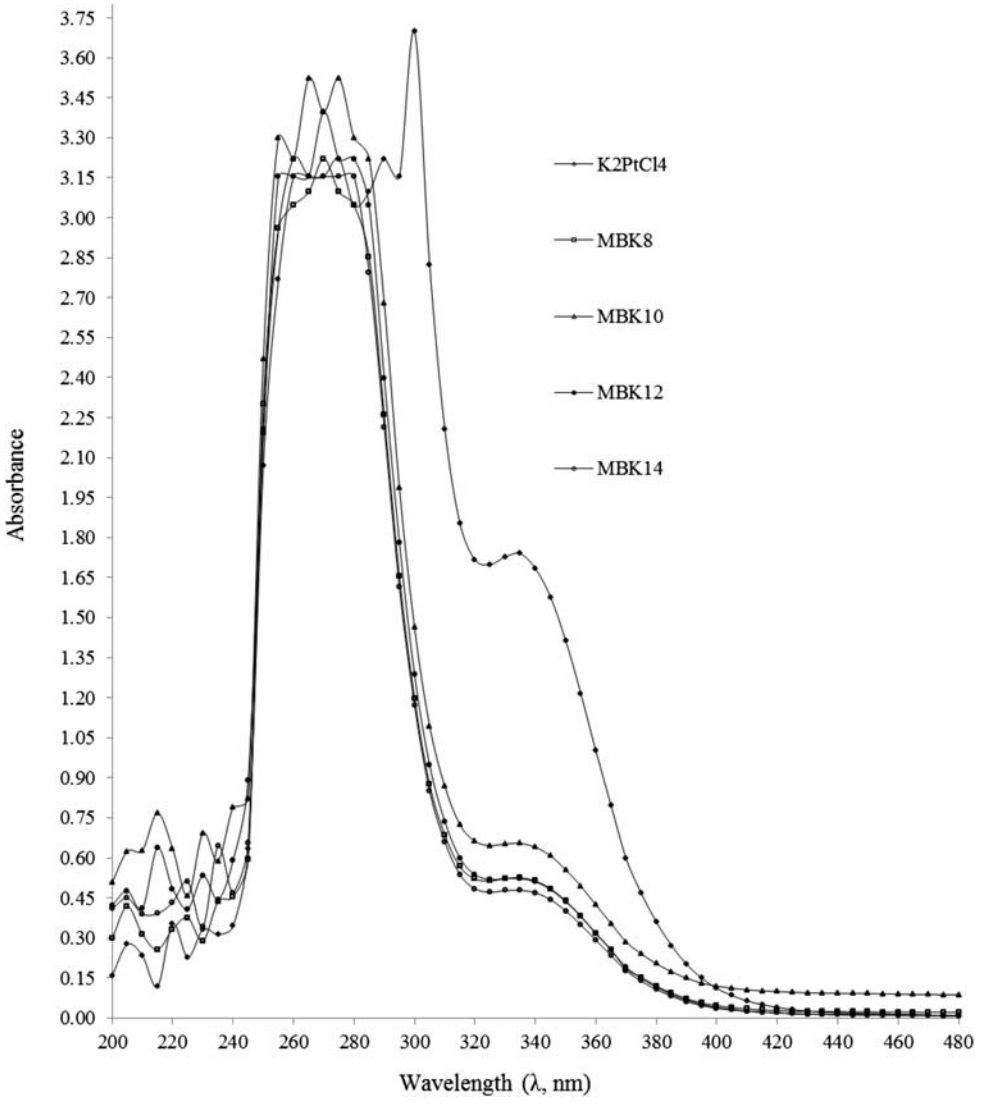

Figure 2. UV/Vis spectra of MBKs in DMSO-water.

that the compounds have assembled into supramolecular frameworks with $[(C_6H_5CH_2N(CH_3)_2(C_nH_{2n+1})]_2^+$ and $[PtCl_4]^{2-}$ (figure 4), similar to the Magnus salt where $[Pt(NH_3)_4]^{2+}$ and $[PtCl_4]^{2-}$ units assemble into a supramolecular structure [19].

3.4. *Molar conductivity analysis*

Low molar conductivities (table 1) were noted, although the compounds are ionic in nature. The Columbic attraction between cationic quaternary ammonium and anionic tetrachloroplatinate is very strong (figure 4), restricting free movement of ions. The compounds exhibited very similar low molar conductivities due to their low electrolytic tendency as evidence of cation–anion interaction (supramolecular interaction).

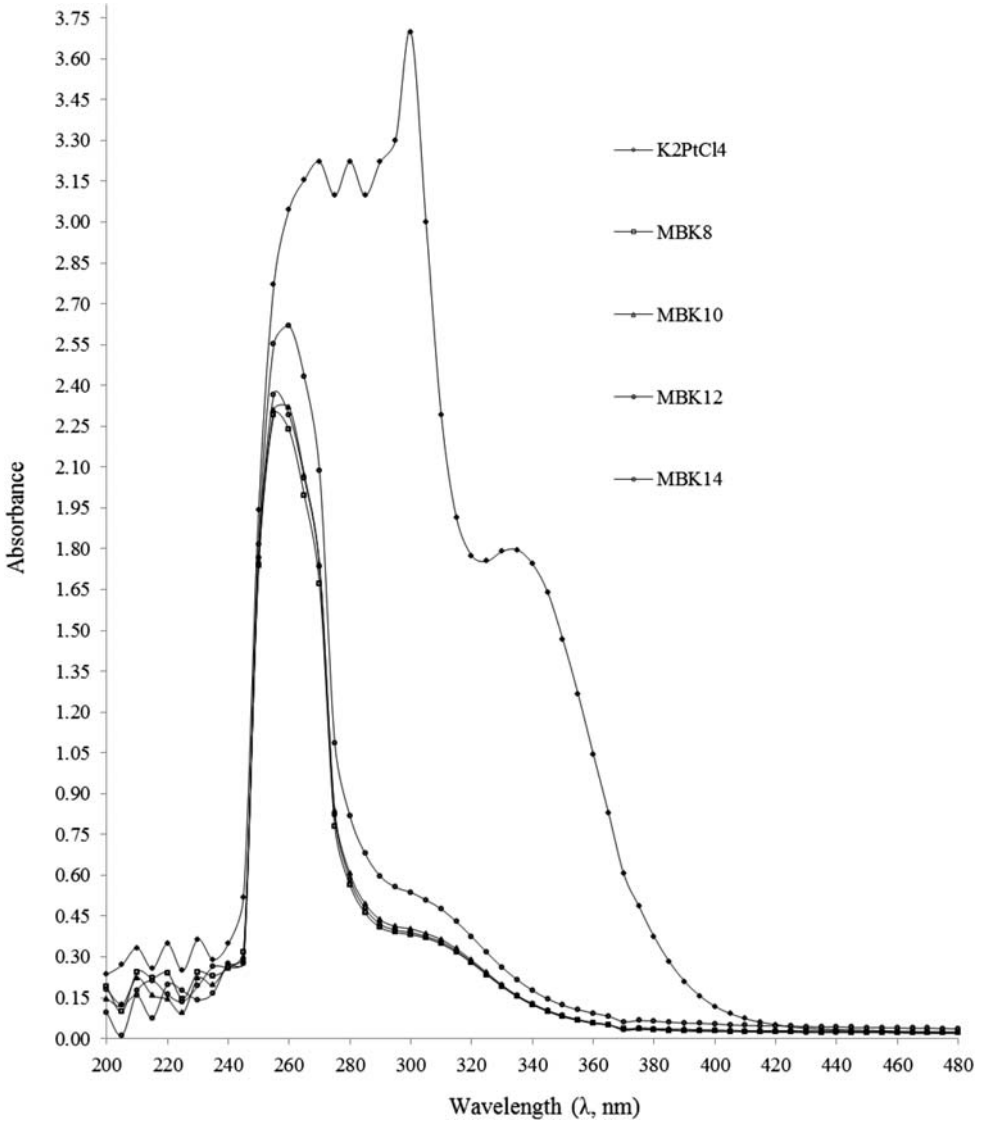

Figure 3. UV/Vis spectra of MBKs in DMSO-phosphate buffer.

3.5. *Zeta potential and particle size measurement*

Zeta potential and particle size distribution were determined with DLS for 15% MBK8 in DMSO and showed 4.56 mv zeta potential with positive polarity, indicating low quantified magnitude of electrical charges at the double layer. Comparing the average value of Zeta potential from the literature [76], MBK8 showed a strong agglomeration as existence of stability. Their distribution is illustrated (Supplementary material) where the particles of 6540 nm are passed 100% through a zero% channel, implying maximum size of 6540 nm and the particle surface obtained as mean area diameter is 706 nm. It indicated an average of particles which is less weighed than the mean volume diameter of coarse particles. An average particle size related to population and

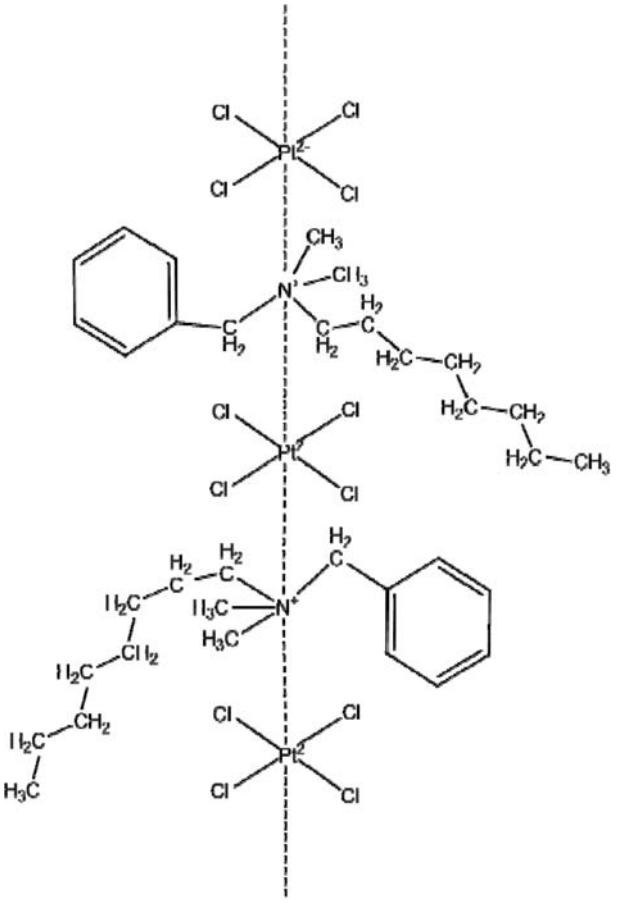

Figure 4. Supramolecular assembly of MBK units.

Table 1. Conductance, molar conductance, and DSC data of the compounds.

Compound	C/M	Con ($\mu S\,cm^{-1}$)	$\Omega^{-1}\,m^2\,mol^{-1}$	Onset (°C)	Peak (°C)	Area (mJ)	ΔH ($J\,g^{-1}$)
MBK-8	1×10^{-3}	52.19	5.219	117.43	120.03	88.677	54.403
MBK-10	1×10^{-3}	54.17	5.417	115.53	117.25	182.484	88.8969
MBK-12	1×10^{-3}	52.98	5.298	86.68	88.69	86.194	47.8867
MBK-14	1×10^{-3}	52.3	5.230	65.66	72.65	96.929	55.3878

volume distribution was measured as mean number diameter as 316.0 nm. A mean diameter of their intensity distribution reflects a relationship of detected light signal at 2106 nm. The 8.50 M^2/CC, specific surface area had depicted smooth, solid and spherical particles. The 1723, a standard deviation, described a width of measured particles size distribution; it did not provide an indication of statistical error.

3.6. *SEM and EDX analysis*

SEM determined a morphological investigation within 6 μm scanning area; here, we mention only the MBK8 image (Supplementary material). The scanning images showed the

same and single kinds of particles. In EDX analysis, the residue observed on the stub only contained strong signals of platinum (Pt), chlorine (Cl), nitrogen (N), and carbon (C) (Supplementary material). No peaks for potassium of K_2PtCl_4 (starting material) or any others indicate 100% purities. In EDX spectra, three lines were obtained for platinum, for chlorine two and one each for carbon and nitrogen. For Pt, the three lines could be explained that it has a larger size with electrons in shells having principle quantum numbers 1–6. The first line has energy near 10 keV due to the electron vacancy in the M shell filled by an electron of the N shell and Mα radiation emitted. Also, a second line at slightly more than 2 keV depicts vacancy of the L shell which is filled by M shell electron and Lα radiation emitted. The same Lα radiation is emitted for chlorine at 3 keV. Lines for Pt, Cl, C, and N obtained below 1 keV due to K electron vacancies are filled by L electron and Kα radiations emitted.

3.7. *Thermal analysis*

DSC analyzes changes in physical properties on increasing temperature with time [77–80], widely used for inspection of polymer, biopolymer, and pharmaceuticals. On temperature change, disruption of molecular forces takes place which depict the nature and stabilization of the compounds [81]. Our compounds showed an effect of alkyl chain on the onset or melting point peak and fusion enthalpy (Supplementary material). Augmentation in alkyl chain with $–CH_2CH_3$ group decreased onset point by 21.02 °C from MBK12 to MBK14, while the difference from MBK8 to MBK10 is 1.90 °C (table 1). On increasing the mass of the compounds by $–CH_2CH_3$, the melting point is decreased. A decrease in onset indicates sensitiveness and cohesivity due to decrease with augmentation of alkyl chain. The ΔH values indicate heat-holding capacities which are MBK10 > MBK14 > MBK8 > MBK12, with maximum value for MBK10. No consequential effect of alkyl chain on ΔH values explains the total heat energy uptake after a suitable transition [82]. A maximum area of MBK10 inferred the strongest cohesivity.

3.8. *Topographical studies*

Topographical images taken with AFM of a thin film coated on a glass slide in 30 μm scan area showed similar images. The image of MBK8 is analyzed (figure 5). An orientation in arrays of coordination planes in $[(C_6H_5CH_2N(CH_3)_2(C_nH_{2n+1})]_2^+$ $[PtCl_4]^{2-}$ units were shown from AFM. Line analysis of topographic image at −231.84 and 236.91 nm showed minimum and maximum values, respectively, in the selected line (table 2). Average value of minimum and maximum is 2.124 nm, a mid value. The root mean square of roughness and average roughness area were 104.133 and 87.345 nm, respectively. The point average roughness area was calculated by 10-point average roughness and was 282.015 nm. Skewness (Rsk) and kurtosis (Rku) values of a line are also shown in table 2, for spikiness of a sample surface.

3.9. *Gas adsorption*

Sorption isotherms for N_2, used in specific surface area and pore structure measurements, have been accurately determined on a number of mineral, oxide, and metallic salt systems

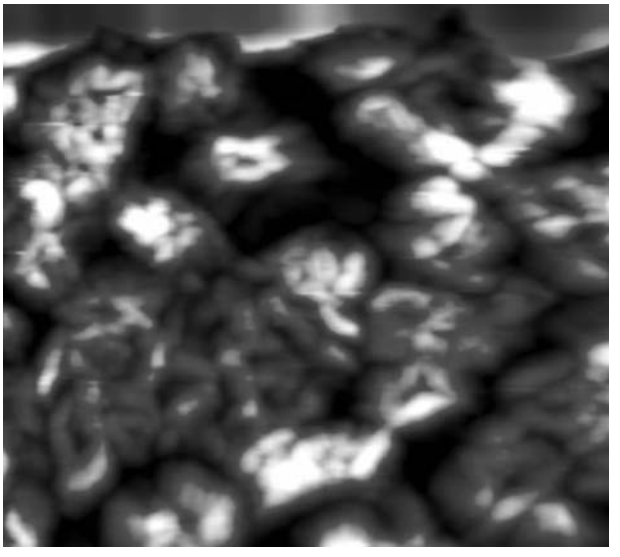

Figure 5. AFM topographic image of MBK8.

Table 2. AFM data for MBK8.

Line	Min (nm)	Max (nm)	Mid (nm)	Mean (nm)	Rpv (nm)	Rq (nm)	Ra (nm)	Rz (nm)	Rsk	Rku
Red	−231.843	236.091	2.124	0	467.935	104.133	87.345	282.015	0.045	2.487

[83]. Specific surface area of MBK8 is obtained by BET, where isotherm (Supplementary material) and pore size distribution (Supplementary material) illustrate that the extent of apparent cross-sectional areas for adsorbed nitrogen vary with surface structure, exchangeable ion, and microporosity. An isotherm obtained for nitrogen on MBK8 surface, where the value of the BET area for the MBK8 was 6.286992 $m^2 g^{-1}$, and the pore size distribution was also obtained for MBK8 (table 3). Specific surface area and pore structure of MBK8 are two of its most important characteristics in determining both its chemical and physical interactions with its surroundings. Experimental studies of such reactions refer back to a unit area basis. Similarly, interpretation of physical properties like swelling behavior, aggregate structure formation, and permeability requires an accurate measurement of specific surface area and pore structure.

3.10. *Antioxidant activities*

Activities were evaluated by free radical-scavenging effect of stable, DPPH as per the literature procedure [84] with slight modifications. The percent scavenging activity of the MBKs was determined in a concentration-dependent manner in comparison to DPPH free radical absorption at 517 nm [85,86] in DMSO/water of 0.440–0.445 absorbance maximum. The addition of synthesized compounds with various concentrations from 0.01 to 4 $\mu g\,mL^{-1}$ showed a decrease in absorption, indicating antioxidant activities (figure 6).

Table 3. BET data for MBK8.

Surface area calculation	
Calculation method	BET
P/P_0	0.007–0.306
Monolayer volume (ncc g^{-1})	1.438074
Specific surface area ($m^2 g^{-1}$)	6.256992
Correlation factor	0.9837337
C value of BET equation	7.595982
Pore-specific volume ($cm^3 g^{-1}$)	0
Pore-specific volume at P/P_0	0.9910728
Pore size calculation	
Calculation method	BJH
Pore size range (diameter)	0.31–1.0
Cumulative volume ($cm^3 g^{-1}$)	0.058
Maximum diameter (nm)	2.784302
Average diameter (nm)	782.7239

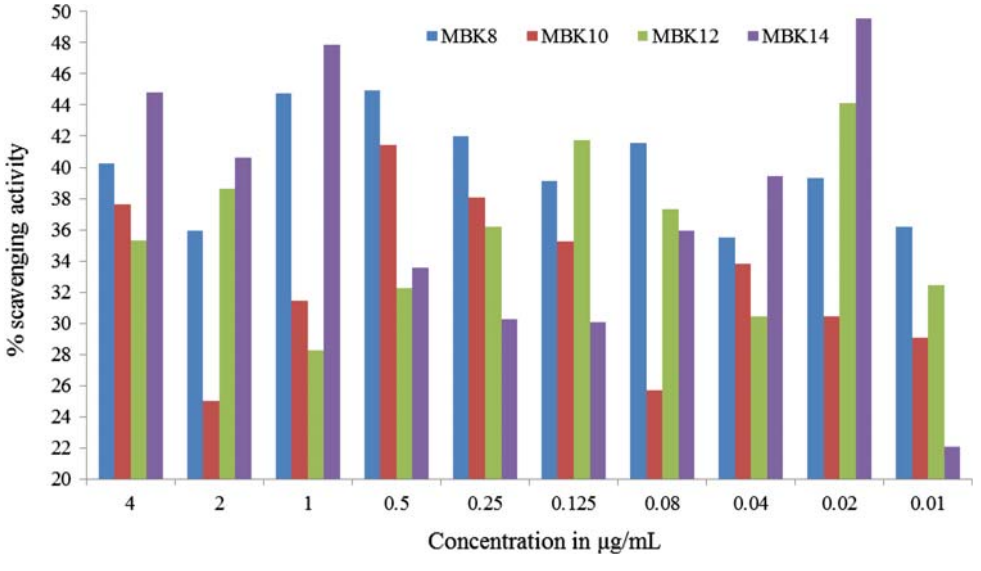

Figure 6. Free radical scavenging activities of MBKs.

MBK8 and MBK10 showed maximum antioxidant nature at 0.5 µg mL^{-1} with 44.94 and 41.43%, respectively, while MBK12 showed at 0.02 µg mL^{-1} with 44.15%. MBK14 showed almost 50% of scavenging activity at 0.02 µg mL^{-1} referred to as its EC_{50} value.

3.11. *Biological evaluation*

Biological evaluation was made by Kirby Beurs Disc Diffusion Method with the literature procedure [86,87]. Due to quaternary nitrogen, MBKs gave best response against Gram-negative *E. coli* and Gram-positive Staphylococci excepting MBK14 (table 4). The MBK12 has 100% zone of inhibition in comparison with standard for Staphylococci, while MBK8 and MBK10 have almost equal zone of inhibitions with 86.66 and 80% against

Table 4. Antibacterial activities for MBKs.

Compound (200 μg)	Zone of inhibition on Staphylococci (mm)	Zone of inhibition on *E.coli* (mm)
MBK8	26	24
MBK10	26	24
MBK12	30	19
MBK14	19	00
Control (standard)	30	20

Staphylococci and *E. coli*, respectively. MBK14 is not effective against *E. coli*. The biological evaluation inferred that with an augmentation in the alkali chain, the MBKs showed greater activity against positive organisms and less against negative organisms.

4. Conclusion

Synthesis and characterization of tetraammoniumplatinates derived from BKC and potassium tetrachloroplatinate were stable under physiological conditions. The platinum-based ionic supramolecular complexes have been obtained through a simple approach of using water as medium at NTP. UV/Vis studies using different media show stability of the compounds. Powder XRD data confirm crystalline nature of the synthesized compounds. The molar conductivities and zeta potential confirmed their ionic supramolecular framework. A larger surface area of MBK8, 6.29×10^4 $cm^2\,g^{-1}$, obtained by BET is important data. The sharper onset temperature areas in DSC data revealed that the complexes have a fixed lattice which does melt at a similar temperature. The compounds exhibited good antimicrobial and antioxidant activities, with best for MBK14 and MBK12. Diffusion coefficients, structural modifications, and other biological studies to determine their role on the apoptotic and proliferate pathways in tumor cell lines continue. Since the complexes belong to a class of supramolecules, intramolecular multiple force theory, and friccohesity could be models for their physicochemical studies.

Supplementary material

It includes SEM/EDX analysis, particle, and pore size distributions separately.

Acknowledgements

Authors are thankful to the Vice Chancellor, Central University of Gujarat, Gandhinagar, for financial, infrastructural support, and experimental facilities.

References

[1] M. Atoji, J.W. Richardson, R.E. Rundle. *J. Am. Chem. Soc.*, **79**, 3017 (1957).
[2] P.B. Chock, J. Halpern, F.E. Paulik, S.I. Shupack, T.P. Deangelis. *Inorg. Synth.*, **28**, 349 (1990).
[3] G. Magnus. *Pogg. Ann.*, **14**, 239 (1828).
[4] G. Magnus. *Ann. Chim. Phys. Sér. 2.*, **40**, 110 (1829).
[5] J. Gros. *Ann. Pharm.*, **27**, 241 (1838).
[6] J. Reiset. *Compt. Rend. Acad. Sci.*, **10**, 870 (1840).

[7] J. Reiset. *Ann. Chim. Phys., Sér. 3*, **11**, 417 (1844).
[8] F.W. Clarke, M.E. Owens. *Am. Chem. J.*, **3**, 350 (1881).
[9] M.L. Rodgers, D.S. Martin. *Polyhedron*, **6**, 225 (1987).
[10] D.S. Martin, R.M. Rush, R.F. Kroening, P.E. Fanwick. *Inorg. Chem.*, **12**, 301 (1973).
[11] M. Peyrone. *Ann. Chem. Pharm.*, **51**, 1 (1844).
[12] S. Yamada. *J. Am. Chem. Soc.*, **73**, 1579 (1951).
[13] V.H. Houlding, A.J. Frank. *Inorg. Chem.*, **24**, 3664 (1985).
[14] K. Honda, K. Chiba, E. Tsuchida, A.J. Frank. *J. Mater. Sci. Lett.*, **24**, 4004 (1989).
[15] V.A. Palkin, T.A. Kuzina, N.N. Kuz.mina, R.N. Shchelokov. *Zh. Neorg. Khim.*, **25**, 1291 (1980).
[16] V.A. Palkin, N.N. Kuz.mina, I.I. Chernyaev. *Zh. Neorg. Khim.*, **10**, 41 (1965).
[17] D. Hunter, R. Milton, K.M.A. Perry. *Br. J. Ind. Med.*, **21**, 92 (1945).
[18] R.D. Murdoch, J. Pepys. *Clin. Exp. Immunol.*, **58**, 478 (1984).
[19] W. Caseri. *Platinum Met. Rev.*, **48**, 91 (2004).
[20] A. Hantzsch, F.Z. Rosenblatt. *Z. Anorg. Allg. Chem.*, **187**, 241 (1930).
[21] T. Yoshida, T. Yamagata, T.H. Tulip, J.A. Ibers, S. Otsuka. *J. Am. Chem. Soc.*, **100**, 1064 (1978).
[22] P. Braunstein, J.-M. Jud, Y. Dusausoy, J. Fischer. *Organometallics*, **2**, 180 (1983).
[23] A.A. Frew, R.H. Hill, L. Manojlovic-Muir, K.W. Muir, R.J. Puddephatt. *J. Chem. Soc., Chem. Commun.*, 198 (1982).
[24] R.J. Goodfellow, I.R. Herbert, A.G. Orpen. *J. Chem. Soc., Chem. Commun.*, 1386 (1983).
[25] M.P. Brown, R.J. Puddephatt, M. Rashidi, L. Manojlovic-Muir, K.W. Muir, T. Solomun, K.R. Seddon. *Inorg. Chim. Acta*, **23**, L33 (1977).
[26] M. Ciriano, J.A.K. Howard, J.L. Spencer, F.G.A. Stone, H. Wadepohl. *J. Chem. Soc., Dalton Trans.*, 1749 (1979).
[27] A. Modinos, P. Woodward. *J. Chem. Soc., Dalton Trans.*, 1516 (1975).
[28] N.J. Taylor, P.C. Chieh, A.J. Carty. *J. Chem. Soc., Chem. Commun*., 448 (1975).
[29] L.V. Interrante, R.P. Messmer. *Inorg. Chem.*, **10**, 1175 (1971).
[30] J.R. Miller. *J. Chem. Soc.*, 4452 (1961).
[31] D.-M. Peyrone. *Ann. Chim. Phys. Sér. 3.*, **16**, 462 (1846).
[32] G.C. Wittstein. *Repertorium Pharm.*, **100**, 456 (1848).
[33] Vauquelin. *Ann. Chim. Sér. 2*, **5**, 260 (1817).
[34] Vauquelin. *Ann. Chim. Sér. 2*, **5**, 392 (1817).
[35] E. Hertel, K. Schneider. *Z. Anorg. Allg. Chem.*, **202**, 77 (1931).
[36] J. Bremi, V. Gramlich, W. Caseri, P. Smith. *Inorg. Chim. Acta*, **322**, 23 (2001).
[37] M. Fontana, H. Chanzy, W.R. Caseri, P. Smith, A.P.H.J. Schenning, E.W. Meijer, F. Gröhn. *Chem. Mater.*, **14**, 1730 (2002).
[38] A.D. Westland, L. Westland. *Talanta*, **3**, 364 (1960).
[39] L.M. Gindin. *Zh. Vses. Khim. O–va*, **15**, 395 (1970).
[40] L.M. Gindin, S.N. Ivanova, A.A. Mazurova, L.Ya. Mironova. *Zh. Neorg. Khim.*, **10**, 502 (1965).
[41] L.M. Gindin, S.N. Ivanova, A.A. Mazurova, A.A. Vasil'eva. *Izv. SOAN SSSR, Ser. Khim. Nauk*, **1**, **2**, 89 (1967).
[42] A.A. Vasil'eva, L.M. Gindin, S.I. Ivanova. *Izv. SOAN SSSR, Ser. Khim. Nauk*, **2**, **4**, 174 (1967).
[43] D.L. Dyer, A. Shinder, F. Shinder. *Fam. Med.*, **3**, 633-S (2000).
[44] K. Green, J.M. Chapman, L. Cheeks, R.M. Clayton, M. Wilson, A. Zehir. *Toxicol. Cut. Ocul. Toxicol.*, **6**, 89 (1987).
[45] B. Grillitsch, O. Gans, N. Kreuzinger, S. Scharf, M. Uhl, M. Fuerhacker. *Water Sci. Technol.*, **54**, 111 (2006).
[46] N.N. Daoud, N.A. Dickinson, P. Gilbert. *Microbios*, **37**, 73 (1983).
[47] G. Debreceni, R. Meggyesi, G. Mestyan. *Br. J. Anaesth.*, **98**, 131 (2007).
[48] S.H. Chung, S.K. Lee, S.M. Cristol, E.S. Lee, D.W. Lee, K.Y. Seo, E.K. Kim. *Mol. Vis.*, **12**, 415 (2006).
[49] F. Brill, P. Goroncy-Bermes, W. Sand. *Int. J. Hyg. Environ. Health*, **209**, 89 (2006).
[50] H.F. Rabenau, G. Kampf, J. Cinatl, H.W. Doerr. *J. Hosp. Infect.*, **61**, 107 (2005).
[51] P. Msellati, N. Meda, V. Leroy, R. Likikouet, P. Van de Perre, M. Cartoux, D. Bonard, A. Ouangre, P. Combe, L. Gautier-Charpentier, F. Sylla-Koko, R. Lassalle, M. Dosso, C. Welffens-Ekra, F. Dabis, L. Mandelbrot. *Sex Transm. Inf.*, **75**, 420 (1999).
[52] M.R. Bray, R.J. Deeth, V.J. Paget, P.D. Sheen. *Int. J. Quantum Chem.*, **61**, 85 (1996).
[53] F.A. Cotton, G. Wilkinson. *Advanced Inorganic Chemistry*, Wiley, New York, NY (1988).
[54] R. Caminiti, M. Carbone, C. Sadun. *J. Mol. Liq.*, **75**, 149 (1998).
[55] W.L. Waltz, J. Lilie, A. Goursot, H. Chermette. *Inorg. Chem.*, **28**, 2247 (1989).
[56] J. Chatt, G.A. Gamlen, L.E. Orgel. *J. Chem. Soc*., 486 (1958).
[57] B.G. Anex, N. Takeuchi. *J. Am. Chem. Soc.*, **96**, 4411 (1974).
[58] L.I. Elding, L.F. Olsson. *J. Phys. Chem.*, **82**, 69 (1978).
[59] D.S. Martin, J.G. Foss, M.E. McCarville, M.A. Tucker, A. Kassman. *J. Inorg. Chem.*, **5**, 491 (1966).
[60] S.B. Piepho, P.N. Schatz, A.J. McCaffery. *J. Am. Chem. Soc.*, **91**, 5994 (1969).

[61] P. Biloen, R. Prins. *Chem. Phys. Lett.*, **16**, 611 (1972).
[62] W.E. Moddeman, J.R. Blackburn, G. Kumar, K.A. Morgan, R.G. Albridge, M.M. Jones. *Inorg. Chem.*, **11**, 1715 (1972).
[63] R.F. Fenske, D.S. Martin, K. Ruedenberg. *Inorg. Chem.*, **1**, 441 (1962).
[64] H.B. Gray, C.J. Ballhausen. *J. Am. Chem. Soc.*, **85**, 260 (1963).
[65] F.A. Cotton, C.B. Harris. *Inorg. Chem.*, **6**, 369 (1967).
[66] H. Basch, H.B. Gray. *Inorg. Chem.*, **6**, 365 (1967).
[67] R.P. Messmer, L.V. Interrante, K.H. Johnson. *J. Am. Chem. Soc.*, **96**, 3847 (1974).
[68] R.P. Messmer, U. Wahlgren, K.H. Johnson. *Chem. Phys. Lett.*, **18**, 7 (1973).
[69] S. Larsson, L.-F. Olsson, A. Rosen. *Int. J. Quantum Chem.*, **25**, 201 (1984).
[70] A. Cristaudo, F. Severino, V. De Rocco, M. Di Lella, E. Picardo. *Allergy*, **60**, 159 (2005).
[71] Y. Sun, S. Gou, R. Yin, P. Jiang. *Eur. J. Med. Chem.*, **46**, 5146 (2011).
[72] K. Nakamoto. *Infrared and Raman Spectra of Inorganic and Coordination Compounds*, Wiley, New York, NY (1970).
[73] W.P. Griflith. *J. Chem. Soc. A*, 899 (1966).
[74] A.D. Allen, C.V. Senott. *Can. J. Chem.*, **45**, 1337 (1968).
[75] L. Trynda, D. Kwiatkowska, W. Tyran. *Gen. Physiol. Biophys.*, **17**, 25 (1998).
[76] L. Obreja, D. Pricop, N. Foca, V. Melnig. *Materiale Plastice*, **1**, 47 (2010).
[77] P. J. Haines, M. Reading, F.W. Wilburn. *Handbook of thermal analysis and calorimetry*, Vol. 1, p. 279, Elsevier Science BV, Amsterdam (1998).
[78] G. Hohne, W. Hemminger, H.J. Flammersheim. *Differential Scanning Calorimetry*, Springer-Verlag, Berlin (1996).
[79] P.L. Privalov, S.A. Potekhin. *Methods Enzymol.*, **131**, 4 (1986).
[80] D.T. Haynie. *Biological Thermodynamics*, Cambridge University Press, Cambridge (2008).
[81] A. Cooper. Microcalorimetry of Protein-DNA Interactions. In *DNA-Protein Interactions - a Practical Approach*, p. 125, Oxford University Press, Oxford (2000).
[82] A. Cooper, M.A. Nutley, A. Walood. Differential Scanning Microcalorimetry. In *Protein-Ligand Interactions: Hydrodynamics and Calorimetry*, S.E. Harding and B.Z. Chowdhry (Eds.), p. 287, Oxford University Press, Oxford (2000).
[83] L.A.G. Aylmore. *Clays Clay Miner.*, **22**, 175 (1974).
[84] J.H. Moon, J. Terao. *J. Agric. Food Chem.*, **46**, 5062 (1998).
[85] A. Ziyad Tahaa, M. Abdulaziz Ajlounia, A.L. Waleed Momanib, A. Abeer, A.L. Ghzawia. *Spectrochim. Acta Part A*, **81**, 570 (2011).
[86] R. Trivedi, S. Bhavya Deepthi, L. Giribabu, B. Sridhar, P. Sujitha, C. Ganesh Kumar, K.V.S. Ramakrishna. *Eur. J. Inorg. Chem.*, 2267 (2012).
[87] W.L. Drew, A.L. Barry, R. O'toole, C.J. Sherris. *Appl. Microbiol.*, 240 (1972).